Copolymerization Propagation Kinetics of Styrene and Methyl Methacrylate-Revisited. 2. Kinetic Analysis

Michelle L. Coote, Lloyd P. M. Johnston, and Thomas P. Davis*

School Of Chemical Engineering & Industrial Chemistry, University of New South Wales, Sydney, NSW 2052, Australia

Received July 15, 1997; Revised Manuscript Received September 30, 1997[⊗]

ABSTRACT: In this work, both the implicit penultimate model and a version of the terminal bootstrap model were fitted to extensive $\bar{k}_p$ data covering a temperature range of 17.9−57.2 °C, for the copolymerization of styrene and methyl methacrylate (STY−MMA). The average activation energies and frequency factors were also calculated for STY−MMA copolymerizations, and the physical meaning of these parameters was explored. Insufficient composition data at the temperatures studied, together with the extreme sensitivity of the fitted model parameters to small errors in the kinetic data and the fixed constants, precluded the attachment of any physical significance to the parameters obtained. Nevertheless, two important conclusions can be drawn from this work. Firstly, there appears to be a temperature effect on the average radical reactivity ratios ($s = s_1 = s_2$), which suggests that there may be an enthalpic component to any penultimate unit effect present. Secondly, it appears that the bootstrap model is not a realistic alternative to the implicit penultimate model for describing the kinetics of ordinary copolymerizations such as STY−MMA.

Introduction

In the preceding paper,[1] we presented the results of a pulsed laser polymerization (PLP) study in which the average propagation rate coefficient, $\bar{k}_p$, was measured for copolymerizations of styrene (STY) with methyl methacrylate (MMA). The objective of this work was to enable sensitive discrimination between the alternative models for copolymerization kinetics. The system STY−MMA was chosen as it is the most widely studied copolymerization and is generally regarded as a typical example of copolymerization behavior in the absence of additional system-specific effects. Although STY−MMA has been widely studied, the available kinetic data are deficient in both quality and quantity for sensitive model discrimination. In compiling our STY−MMA data we attempted to address these problems by (1) combining the technique of PLP with direct methods of molecular weight analysis, (2) compiling the largest set of $\bar{k}_p$ data to date for this system, and (3) compiling the data at five different temperatures. It was hoped that through (1) and (2) we could reduce the uncertainty in the parameter estimates obtained by fitting the different models to the data, enabling via (3) a careful study of their temperature dependence, which would thus enable more sensitive testing of the alternative models than has previously been possible.

In this paper, the results of this kinetic analysis will be presented. We first outline the different models for copolymerization kinetics, then describe the statistical procedures used, and finally present the results of the analysis. This analysis is split into four main parts: (1) fitting of the implicit penultimate model to composition and sequence distribution data for STY−MMA; (2) fitting of the implicit penultimate model to $\bar{k}_p$ data for STY−MMA; (3) fitting of a version of the terminal bootstrap model to the $\bar{k}_p$ data; (4) calculation of the Arrhenius parameters for the different copolymerizations of STY−MMA.

[⊗] Abstract published in *Advance ACS Abstracts,* December 15, 1997.

Models for Copolymerization Kinetics

Models for copolymerization kinetics take a set of assumptions regarding the factors influencing the reactivity of the propagation step and, invoking the long-chain assumption and the quasi-steady-state assumption, predict the expected copolymer composition, microstructure, and k_p as a function of the molar fractions (f_1 and f_2) of each of the comonomers in the feed and a set of characteristic constants. In this paper two such models will be considered: the implicit penultimate model and a version of the terminal bootstrap model. These two models are considered the most likely contenders to replace the terminal model as a general description of copolymerization kinetics. In what follows, we will first outline these three models (the terminal model, the implicit penultimate model and the terminal bootstrap model) and then explain the intended model discrimination procedure.

Terminal Model. The simplest copolymerization model is the terminal model, which assumes that the reactivity of the terminal unit of a polymer radical is the only factor influencing its reactivity in propagation or transfer reactions. The (low conversion) terminal model equations for predicting copolymer composition and $\bar{k}_p$ are as follows.

$$\frac{F_1}{F_2} = \frac{f_1}{f_2}\frac{r_1 f_1 + f_2}{r_2 f_2 + f_1} \tag{1}$$

$$\bar{k}_p = \frac{r_1 {f_1}^2 + 2 f_1 f_2 + r_2 {f_2}^2}{[r_1 f_1/k_{11}] + [r_2 f_2/k_{22}]} \tag{2}$$

where f_1 and f_2 are the molar fractions of the monomers in the feed, F_1 and F_2 are the molar fractions of the monomers in the copolymer, and k_{11} and k_{22} are the homopropagation rate coefficients. In these equations, there are four characteristic constants: two homopropagation rate coefficients (k_{ii}) and two reactivity ratios (r_i). The latter are defined as follows.

$$r_i = \frac{k_{ii}}{k_{ij}} \quad \text{(where } i \neq j \text{ and } i, j = 1 \text{ or } 2\text{)} \tag{3}$$

S0024-9297(97)01052-8 CCC: $14.00

For many years this terminal model was believed to be the basis model for copolymerization kinetics because it could describe the composition of most copolymerization systems tested. It is true that exceptions to the terminal model were known, and more complex copolymerization models were derived for these systems by taking into account additional influences on radical reactivity. These additional influences can be loosely grouped into three main categories:

(1) Additional units (though typically only the penultimate unit) in the polymer chain are also assumed to influence the radical reactivity.

(2) Some form of monomer partitioning is assumed to be present, thereby causing deviations from the expected kinetic behavior by causing a discrepancy between the measured (overall) monomer fractions and those in the vicinity of the active chain end (this is known as a bootstrap effect).[2]

(3) Some additional reaction (such as depropagation or complex formation between the comonomers and/or the radical) is assumed to be occurring, thereby complicating the overall propagation rate.[3]

While there was strong evidence for many of these effects in certain specific systems, these were regarded as exceptional and the terminal model was held to be the basis model of copolymerization kinetics.

However, in 1985 Fukuda et al.[4] measured the $\bar{k}_p$ for STY−MMA copolymerizations—a system that was previously believed to obey the terminal model—and found that while its composition was well described by the terminal model its k_p was not. This result was verified by other workers—both for STY−MMA[5,6] and many other copolymerization systems[7−11]—and it now appears that this is a general phenomenon in free radical copolymerization kinetics. To describe this behavior, the models originally reserved for the exceptional systems were reconsidered as a general description of copolymerization kinetics. Of the alternative models listed above, (1) and (2) seem the most likely to describe the basis of copolymerization kinetics, as there is no evidence to suggest that reactions such as depropagation and complex formation occur in systems such as STY−MMA (at least within the temperature ranges studied). Hence we will concentrate on these two alternatives for the remainder of this work.

Implicit Penultimate Model. The terminal model may be extended by assuming that additional units in the polymer chain influence the reactivity of a growing polymer radical, and the simplest such extension to the terminal model is the penultimate model. In the general penultimate unit model[12] it is held that both the terminal and penultimate units influence the radical reactivity. Equations for the penultimate model are obtained by replacing the characteristic constants of the terminal model (that is, the monomer reactivity ratios, r_1 and r_2, and the "homopropagation rate coefficients", k_{11} and k_{22}) by average quantities, defined as follows:

$$\bar{r}_i = r_i'\left(\frac{f_i r_i + f_j}{f_i r_i' + f_j}\right) \tag{4}$$

$$\bar{k}_{ii} = k_{iii}\left(\frac{r_i f_i + f_j}{r_i f_i + f_j/s_i}\right) \tag{5}$$

where $i \neq j$ and $i, j = 1$ or 2. In place of the four characteristic constants of the terminal model, there are eight characteristic constants in the penultimate model: the two homopropagation rate coefficients (k_{iii}), four monomer reactivity ratios (r_i and r_i'), and two radical reactivity ratios (s_i). The monomer and radical reactivity ratios are defined as follows.

$$r_i = \frac{k_{iii}}{k_{iij}} \tag{6}$$

$$r_i' = \frac{k_{jii}}{k_{jij}} \tag{7}$$

$$s_i = \frac{k_{jii}}{k_{iii}} \tag{8}$$

where $i \neq j$ and $i, j = 1$ or 2.

Now, the above expressions are used to describe penultimate unit effects on both copolymer composition and microstructure, as well as $\bar{k}_p$. In order to describe systems such as STY−MMA, for which the composition and microstructure could be described by a terminal model, Fukuda et al.[4] suggested that the following restriction be placed on the penultimate model.

$$r_i\left(=\frac{k_{iii}}{k_{iij}}\right) = r_i'\left(=\frac{k_{jii}}{k_{jij}}\right) \tag{9}$$

where $i \neq j$ and $i, j = 1$ or 2. With this restriction, the penultimate unit effect would only appear in values of the radical reactivity ratios and, since these constants only appear in the $\bar{k}_p$ equation, the composition and microstructure equations of the penultimate model collapse to their terminal model forms. This restricted penultimate unit effect is known as an *implicit* penultimate unit effect (IMPUE) so as to distinguish it from the general or *explicit* penultimate unit effect (EPUE).[13] It should be noted that in making the above restriction, it is implicitly assumed that the magnitude of the penultimate unit effect is independent of the reacting monomer, for the equality $k_{jii}/k_{iii} = k_{jij}/k_{iij}$ follows from the assumption that $r_i = r_i'$.

Although this implicit penultimate model is able to describe existing copolymerization data, two problems have emerged. Firstly, the theoretical basis for the restriction on the penultimate unit effect has been a matter of contention. To date, two alternative accounts of the origin of the IMPUE have been suggested—known as the enthalpic and entropic models. In the enthalpic model, suggested by Fukuda et al.,[14] it is proposed that the penultimate unit affects only the stability of the reacting radical but is too far away to interact with the reacting monomer. In this way, the penultimate unit would (via an Evans−Polanyi rule) affect the activation energy, but the effect would be independent of the reacting monomer. In the entropic model, suggested by Heuts et al.,[15] it is proposed that the penultimate unit affects the frequency factor of the propagation reaction but, provided the two monomers are not too dissimilar in size, the effect cancels from the monomer reactivity ratios and appears only in the radical reactivity ratios. To date, discrimination between these two alternative mechanisms has not been possible because they predict the same type of kinetic behavior and differ only in their predicted values of the radical reactivity ratios. Unfortunately, as shown in a previous publication,[16] previous measures of radical reactivity ratios have been subject to considerable uncertainty, which has rendered

impossible any model discrimination based upon their point estimates.

Secondly, it was suggested by Moad et al.[17] that the restriction on the penultimate model may be unnecessary since a general penultimate model can also describe existing kinetic data for systems such as STY−MMA. Given that it is the restriction on the penultimate unit effect (rather than the penultimate unit effect itself) that is difficult to account for theoretically, the general penultimate model might in fact be favored as a chemically simpler alternative to the restricted penultimate model, despite its additional adjustable parameters. The ability of the terminal model to describe the sequence distribution data of systems such as STY−MMA,[18] in addition to its well established ability to describe the composition of these copolymerizations, has led most workers[4−11] to favor the restricted penultimate model over the general penultimate model. For this reason, we will consider only the implicit penultimate model in this work and use the $\bar{k}_p$ data to examine the two alternative accounts of the implicit penultimate unit effect. However, the general penultimate model cannot be ruled out as an alternative to the implicit penultimate model and we recommend that further experiments (for instance the collection of more extensive sequence distribution data) be aimed at discriminating between these two models.

Terminal Bootstrap Model. An alternative means of extending the terminal model is via the inclusion of a bootstrap effect. A bootstrap effect[2] is said to occur if some form of monomer partitioning causes the monomer concentrations in the vicinity of the active chain end to differ from the measured bulk concentrations, thereby causing deviations from the predicted kinetic behavior. Although the bootstrap model was originally derived to account for the effect of an added solvent on homo- and copolymerization reactions, a form of the model may also be derived for bulk copolymerizations. In a bulk copolymerization overall partitioning of monomer is not possible (that is, the sum of the molar fractions of the comonomers in any part of the solution is always unity); however, the relative fractions of the two monomers may differ between the bulk solution and the active chain end. In its simplest form, this form of monomer partitioning may be described by the following equilibrium expression.

$$\frac{f_1}{f_2} = K\left(\frac{f_{1\text{bulk}}}{f_{2\text{bulk}}}\right) \tag{10}$$

where f_1 and f_2 are the molar feed fractions of monomers 1 and 2 at the propagating chain end, $f_{1\text{bulk}}$ and $f_{2\text{bulk}}$ are the bulk (measured) molar feed fractions of monomers 1 and 2, and K is an equilibrium constant. Using this expression to eliminate f_1 and f_2 from the (low conversion) terminal model composition and $\bar{k}_p$ equations, equations for the (low conversion) terminal bootstrap model may be derived:

$$\frac{F_1}{F_2} = \left(\frac{Kf_{1\text{bulk}}}{f_{2\text{bulk}}}\right)\frac{Kf_{1\text{bulk}}r_1 + f_{2\text{bulk}}}{r_2 f_{2\text{bulk}} + Kf_{1\text{bulk}}} \tag{11}$$

$$\bar{k}_p = \left(\frac{1}{f_{2\text{bulk}} + Kf_{1\text{bulk}}}\right)\frac{r_1(Kf_{1\text{bulk}})^2 + 2Kf_{1\text{bulk}}f_{2\text{bulk}} + r_2 f_{2\text{bulk}}^2}{[r_1 Kf_{1\text{bulk}}/k_{11}] + [r_2 f_{2\text{bulk}}/k_{22}]} \tag{12}$$

Examining these equations, it is evident that the bootstrap effect (as measured by the equilibrium constant K) is always aliased with the molar fraction of one of the monomers. Hence, the presence of a bootstrap effect will not cause any *apparent* deviation from the terminal model composition equation (as the composition equations for these two models have the same functional form) but it will affect the kinetics (as the $\bar{k}_p$ equations for the two models are different). Thus the model may be used to describe the behavior of systems such as STY−MMA for which the composition appears to follow a terminal model but the $\bar{k}_p$ does not, and in fact this model was fitted by Maxwell et al.[18] to the STY−MMA composition and $\bar{k}_p$ data of Fukuda et al.[4] They showed that this model was capable of describing the data and that discrimination between this terminal bootstrap model and the implicit penultimate model was not possible (at least for that particular data set).

While this model can describe existing data, it, like the implicit penultimate model, is constrained by a restriction that is difficult to account for theoretically. In the above version of the terminal bootstrap model it is assumed that the partitioning constant K is independent of the feed ratio of the two monomers. Assuming that the partitioning is caused by some interaction between the comonomers and the growing polymer chain, it is likely that the extent of partitioning will be in some way dependent upon the composition of the monomer mixture and/or the growing polymer radical. However, more physically realistic bootstrap models, which allow the partitioning constant to vary as a function of f_1, lead to more complicated models in which both the composition and $\bar{k}_p$ equations differ significantly from the terminal model equations. It is true that, since these more complicated models have extra adjustable parameters, they can often be made to fit available composition data. For instance, Maxwell et al.[18] successfully fitted the STY−MMA composition and $\bar{k}_p$ data of Fukuda et al.[4] with a terminal bootstrap model based upon the following equilibrium expression.

$$\frac{f_1}{f_2} = K\left(\frac{f_{1\text{bulk}}}{f_{2\text{bulk}}}\right)^z \tag{13}$$

where z is an additional adjustable parameter.

However, if we assume that the terminal model does provide a good description of the composition and microstructure of ordinary copolymerizations (such as STY−MMA), then these complex bootstrap models are not convincing alternatives to the implicit penultimate model for providing the basis model for free-radical copolymerization kinetics. For this reason, these complex bootstrap models will not be considered here. However, when more extensive composition and sequence distribution data becomes available, we recommend that they be reconsidered, together with the general penultimate model, for more sensitive model discrimination.

Proposed Model Discrimination Procedure. In summary, while the terminal model can describe the composition and sequence distribution of ordinary copolymerization systems such as STY−MMA, it cannot describe the kinetics of the propagation reaction and is thus no longer accepted as the basis of free-radical copolymerization kinetics. In its place, two alternative models have been suggested: the implicit penultimate model and a version of the terminal bootstrap model.

There are three problems with these alternative models. (1) Since both of these models have several adjustable parameters, they can both be fitted to existing kinetic data and discrimination between them has not yet been possible. (2) In order that their composition equations behave like the terminal model, the parameters of both models are restricted and a theoretical basis for these restrictions has not yet been established. (3) More complex versions of the above models—in which the restrictions are removed—can also be fitted to the existing data, and these cannot be ruled out as alternative descriptions of free-radical copolymerization kinetics. In this work, it was hoped to discriminate between the terminal bootstrap model and the two versions of the implicit penultimate model by examining the physical significance of the fitted model parameters, thereby simultaneously addressing problems (1) and (2). For the remainder of this work, problem (3) will be ignored. However, we recommend that extensive composition and sequence distribution data (at several temperatures) be collected for both STY−MMA and other copolymerizations that appear to obey the terminal model composition equation, in order to address this problem and identify the basis model for copolymerization kinetics.

The procedure for testing the physical significance of the fitted model parameters is as follows. In a previous paper[1] we published the most accurate and extensive $\bar{k}_p$ data to date for copolymerizations of STY−MMA. In this work, the terminal bootstrap and implicit penultimate models will be fitted to this data, and the temperature dependence of the fitted model parameters will be studied. Now, in each of the alternative copolymerization models the fitted model parameters are assigned a physical meaning. Given this physical meaning, the expected temperature dependence of the parameters for each of these three models may be summarized as follows. For the terminal bootstrap model, the monomer reactivity ratios (r_1 and r_2) would be expected to be slightly temperature dependent (since, assuming they have an enthalpic component, $\ln(r_i)$ varies inversely with temperature), while the bootstrap effect (K), being an equilibrium constant, would be expected to be temperature dependent—although the nature of this temperature dependence would depend on the exothermicity of the physical process (or chemical reaction) that caused the partitioning, since $\ln(K) = -\Delta G°/(RT)$. For the implicit penultimate model, the radical reactivity ratios would be expected to be either slightly temperature sensitive (enthalpic model) or insensitive (entropic model) to temperature, depending upon whether or not they have an enthalpic component. By comparing the measured temperature dependence of the fitted model parameters with that expected given their physical meaning, it was hoped to critically test the terminal bootstrap model and the two versions of the implicit penultimate model. The results of this analysis will be presented in this paper. We first fit the implicit penultimate model to composition and sequence distribution data for STY−MMA, and then, using the monomer reactivity ratios obtained, fit the model to the $\bar{k}_p$ data at the different temperatures. Following this, the terminal bootstrap model will also be fitted to the $\bar{k}_p$ data at the different temperatures. In each case we will compare the temperature dependence of the parameters with the expected results.

In addition to studying the temperature dependence of the fitted model parameters, the $\bar{k}_p$ data for STY−MMA copolymerizations will also be used to estimate the Arrhenius parameters. It was hoped to discriminate between the implicit penultimate and terminal bootstrap models by examining the ability of the Arrhenius relationship to fit this data. Furthermore, by studying the variation of the Arrhenius parameters as a function of the monomer feed ratios, it was hoped that discrimination between the enthalpic and entropic models would be possible. In this paper we present the results of this analysis and discuss the physical meaning of the Arrhenius parameters for the overall propagation step of a free-radical copolymerization.

Statistical Analysis Procedures. The fitting procedure used in this work is nonlinear least squares analysis.[19] In this method, the optimum parameters of a model are those which minimize the weighted sum of squares of residuals (SS), as given by

$$\mathrm{SS} = \sum_{i=1}^{n} \left(\frac{y_i = y(x_i)}{\sigma_i} \right)^2 \tag{14}$$

In this equation n is the number of data points and σ_i is the standard deviation of the error distribution in each measured value y_i. The approximate $(1 - \alpha)100\%$ joint confidence interval (JCI) for the parameters obtained is defined by the following formula:

$$\mathrm{SS}(\theta) \le \mathrm{SS}(\theta_o)\left(\left(1 - \frac{p}{n-p}\right)F(p,n-p,1-\alpha)\right) \tag{15}$$

In this formula θ is a vector of p parameters, and θ_o is the vector of the p parameters that minimize the SS. Parameter combinations θ that satisfy this formula lie inside the JCI, and those that do not lie outside. The programs for implementing these formulas were written using the software package *Matlab*. The nonlinear regression program utilized a built-in function minimizer (called "fmins") for minimizing SS with respect to the parameter estimates. This minimizer used a simplex search method and so, in order to ensure that global and not merely local minima were located, each nonlinear regression analysis was repeated with different initial parameter estimates.

The assumptions inherent in this statistical analysis procedure and their relationship to the accurate and precise measurement of radical reactivity ratios have been discussed in detail in a previous publication[16] and may be summarized as follows. Firstly, it assumed that the error in the independent variable is negligible with respect to the dependent variable. For this work, this is a reasonable assumption because the error in the dependent variables ($\bar{k}_p$, composition and sequence distribution), as measured from replicate samples, varies according to the data set but is of the order 5−20%, while the error in the independent variables (f_1 and temperature), as estimated from the limits of reading of the analytical balance used to prepare samples and the thermocouple used to measure the temperature, is less than 1%. Secondly, it is assumed that error in the dependent variable is independently random and normally distributed about the true model. The validity of this assumption was ensured by minimizing systematic errors in the experiments (through measures such as careful calibration of the SEC equipment) and by repeating replicate samples in full (and thus avoiding shortcuts in the experiments such as the preparation of stock solutions). There was one exception to this second precaution. In the measurement of $\bar{k}_p$, three

types of molecular weight analysis of the PLP samples were used to obtain three estimates of $\bar{k}_p$ for the same polymer sample, and the error in these three estimates of $\bar{k}_p$ was not completely independent. However, since the bulk of the error in the measured $\bar{k}_p$ data arises from the molecular weight analysis and not the PLP experiment itself, even when these multiple estimates of $\bar{k}_p$ were combined as part of the same data set, the assumption of independent errors was judged to be reasonable.

A final issue regarding the statistical analysis procedure concerns the weighting of residuals. In the method of nonlinear least squares analysis, the sum of squares is weighted by the inverse of the variance of the error in each data point so that samples with a large error variance do not unfairly bias the analysis. As shown previously,[16] failure to weight the residuals correctly leads to incorrect parameter estimates. In what follows, we will explain the weighting procedure selected for the different types of data analyzed in this work.

In the reanalysis of previously measured composition and sequence distribution data, the data were weighted according to the inverse of the dependent variable (which is equivalent to assuming that the relative error was constant in each of the data sets). This is because for three of the four data sets, the authors[4,18] suggested that the relative error was constant for their data. In original analysis of the fourth set, the authors[20] used unweighted residuals in the statistical analysis of their data (and thus implicitly assumed that the absolute error was constant). However, their data were obtained using exactly the same procedure as that used by one of the authors[18] and was thus likely to have a similar error structure. In the analysis of our own composition data, the standard deviation of the replicates at each of the two monomer feed ratios was used to weight the data. However, when this data was combined with the other four data sets in order to obtain an overall estimate of the monomer reactivity ratios, constant relative error was assumed for all data points. This was because it was difficult to make an accurate judgment about the relative sizes of the error in the different data sets—measured by different people and using different techniques—and so it was decided that this assumption was the least likely to unfairly bias the analysis.

In the analysis of the $\bar{k}_p$ data in this work, the residuals were weighted according to the inverse of the laser repetition rate in the PLP experiment since, as explained in our previous paper,[1] the error in $\bar{k}_p$ data is approximately proportional to this quantity. It is true that the error variance may also be estimated directly from the standard deviation of replicate samples. However, since many of these replicates were produced at different laser repetition rates, in most cases the number of true replicates at each point was only two or three—a number too small for obtaining a reasonable measure of the error variance. When the $\bar{k}_p$ values measured by the three different molecular weight analysis techniques (LALLS, DV, and DRI) were combined in single data set, a further judgment had to be made concerning the relative weighting of data measured by each of these techniques. Since, as will be seen shortly, there are small systematic differences between the data sets and it is impossible to know which of these sets was the most accurate, it was decided to treat all sets equally and simply weight the data as the inverse of the laser repetition rate.

Determination of the Monomer Reactivity Ratios for STY−MMA. In this work, the radical reactivity ratios (s_1 and s_2) are to be measured by fitting the $\bar{k}_p$ equation of the implicit penultimate model to sets of $\bar{k}_p$ vs f_1 data. Now, this equation contains six adjustable parameters—the monomer reactivity ratios (r_1 and r_2), the two homopropagation rate coefficients (k_{111} and k_{222}), and the two radical reactivity ratios. Strictly speaking, all six of these parameters should be simultaneously optimized in the regression procedure. However, since fitting a model with six parameters to relatively small data sets generally leads to indeterminate results, and since the resulting six-dimensional 95% JCIs obtained are difficult to interpret, a two-parameter analysis has been adopted. In this procedure, the monomer reactivity ratios are obtained by fitting the terminal model (and hence the implicit penultimate model) to composition and/or sequence distribution data, and the homopropagation rate coefficients are measured separately in PLP studies of homopolymerizations. These parameters are then used as fixed constants in the regression analysis of the $\bar{k}_p$ data. Now, as noted previously,[16] the resulting two-dimensional 95% JCIs for radical reactivity ratios that are obtained from such an analysis underestimate their true uncertainty, since the analysis fails to take into account the uncertainty in the fixed parameters. However, in this work we will address this problem and estimate the true uncertainty in the radical reactivity ratios, through sensitivity analysis.

To implement the two-parameter analysis described above, we first need to obtain values of the monomer reactivity ratios for STY−MMA. Since reactivity ratios contain an enthalpic component, they are temperature dependent. However, this temperature dependence is often ignored in kinetic studies as, over a temperature range such as this (17.6−57.2 °C), its effect will only be slight. However, for this work we will be examining the temperature dependence of the kinetic behavior, and we therefore need to avoid the possibility of any systematic errors being introduced through such assumptions. Hence we will first examine the temperature dependence of the monomer reactivity ratios for STY−MMA over the range 17.6−57.2 °C. For this study, it was only necessary to measure the monomer reactivity ratios of STY−MMA at a low temperature (20 °C was selected), since there have been recent careful measurements of the monomer reactivity ratios of STY−MMA at both 40[4,18] and 60 °C.[20,21] In what follows, the measurement of the composition of copolymers of STY−MMA, prepared at 20 °C,will be described, and then this data and that of the previous studies will be analyzed in order to estimate the temperature dependence of the monomer reactivity ratios of STY−MMA.

Experimental Section

Materials. STY and MMA were passed through a column of activated alumina (Aldrich) and refrigerated until required. The initiator 2,2′-azobis(isobutyronitrile) (AIBN) was purchased from BDH and used as received. The solvent for the NMR samples was HPLC Grade CCl_4 (Aldrich). The solvent ($CHCl_3$) and precipitant (MeOH) for respectively purifying and recovering the polymer samples were purchased from Ajax Chemicals and Jaegar Chemicals, respectively.

Experimental Design. Tidwell and Mortimer[22] showed that, provided the terminal model could be assumed to be correct, the most sensitive measurements of reactivity ratios from composition data are obtained when the composition of copolymers is measured at two characteristic feed compositions, as given by the following formulas.

$$f_1 = \frac{2}{2 + r_1} \quad \text{and} \quad f_1 = \frac{r_2}{2 + r_2} \tag{16}$$

Assuming the monomer reactivity ratios of Fukuda et al.,[4] for STY−MMA these optimum feed compositions are approximately $f_1 = 0.187$ and $f_1 = 0.793$. Hence these two feed compositions were selected for study in this work, and five samples were prepared at each.

Polymerizations. Purified monomer and initiator (5 mmol/L) were charged to Pyrex sample tubes (10 mm diameter by 60 mm height), deareated by bubbling with argon for 5 min and sealed with rubber septa. The reaction mixtures were shaken vigorously before immersion in a constant temperature bath that was set at the reaction temperature, 20 °C. Samples were left in this bath for 1 week before being precipitated into methanol and dried in a vacuum oven. Samples were purified of any residual monomer by a reprecipitation technique in which they were dissolved in chloroform, then reprecipitated into methanol, and redried in the vacuum oven. The conversion was then checked and was found to be less than 5% for all samples.

NMR Analysis. The ^{1}H NMR spectra of the STY−MMA copolymers (dissolved in CCl_4) were recorded on a Bruker AC-300F spectrometer at a temperature of 300 K. The data were reported in parts per million from internal tetramethylsilane on the δ scale. The instrument parameters were optimized for the accurate measurement of peak integrals. The composition of the STY−MMA copolymers (as measured by the molar fraction of styrene units in the copolymer) was determined from the NMR spectra by multiplying the integral of the aromatic protons of the styrene units by a factor of 8/5 and then dividing this quantity by the sum of the integrals for all of the protons.

Results and Analysis

The composition of the STY−MMA samples is given in Table 1. Using the standard deviation of the replicates at each feed composition to weight the data, the terminal model composition equation (and hence the implicit penultimate model) was fitted to the data in order to estimate the monomer reactivity ratios for STY−MMA at 20 °C. The monomer reactivity ratios obtained were $r_1 = 0.3908$ and $r_2 = 0.5057$. A 95% JCI for these reactivity ratios is given in Figure 1. Also plotted in Figure 1 are the 95% JCIs for the monomer reactivity ratios obtained by reanalyzing the composition data of Fukuda et al.[4] and Maxwell et al.[18] and the sequence distribution data of Burke et al.[20] and Maxwell et al.[18] The sequence distribution data were analyzed using the same peak assignments as those used by both Maxwell et al.[18] and Burke et al.,[20] and these, together with the terminal model equations for the triad fractions, may be found in the original paper by Maxwell et al.[18] The sequence distribution data consisted of six peak fractions for each sample: three fractions for the STY-centered triads and three for the MMA-centered triads. It was noted by Burke et al.[20] that, since the sum of the peak fractions for the STY fractions and the MMA fractions must each add to unity, only four of these fractions are linearly independent, and thus only four fractions (two for each of the STY and MMA fractions) should be used in the analysis. However, when we adopted this recommendation, indeterminate JCIs were obtained and so, as in the analysis of Maxwell et al.,[18] all six fractions were used to determine the monomer reactivity ratios.

Examining the JCIs plotted in Figure 1, it is seen that all of the 95% JCIs overlap each other and there is no obvious trend in the data. This is also seen in Table 2, which lists the point estimates for the monomer reactivity ratios obtained from the analysis of the different data sets. Hence, at a 95% level of confidence the temperature dependence of the monomer reactivity ratios of STY−MMA cannot be measured from this data. Now, based on chemical grounds there is likely to be a temperature effect on the monomer reactivity ratios of STY−MMA. For, the activation energies of the homopropagation and cross-propagation reactions for the monomers STY and MMA are likely to be different. Furthermore, as shown in a previous publication,[16] values of the radical reactivity ratios are extremely sensitive to small changes in the monomer reactivity ratios. Hence, it is likely that, although the temperature dependence of the monomer reactivity ratios cannot be measured from these data, the failure to correct the monomer reactivity ratios for this temperature dependence may introduce a significant systematic error in the measured values of the radical reactivity ratios.

In order to address this problem, all five data sets were combined and analyzed in order to find an overall estimate for the monomer reactivity ratios of STY−

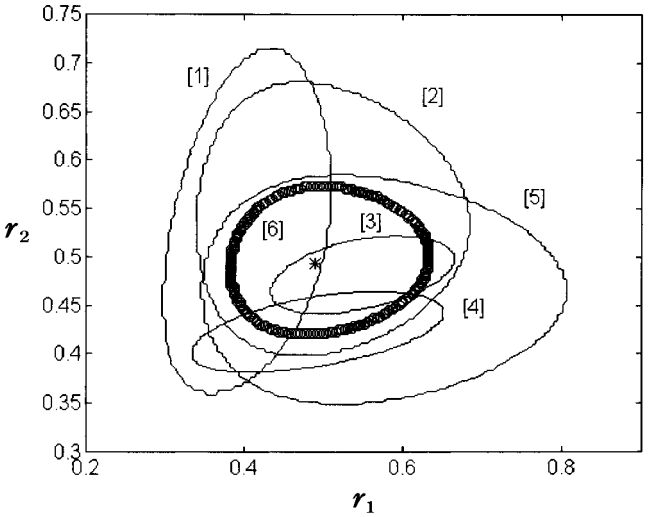

Figure 1. 95% JCIs for the monomer reactivity ratios of STY−MMA as measured from the data of [1] this work (20 °C), [2] Burke et al.[20] (60 °C), [3] Fukuda et al.[4] (40 °C), [4] Maxwell et al.[18] (40 °C composition data), and [5] Maxwell et al.[18] (40 °C sequence distribution data). Also shown is [6] the 95% JCI for the combined data.

Table 1. Composition of STY−MMA at 20 °C

molar fraction of STY in feed, f_1	molar fraction of STY in copolymer, F_1
0.186	0.304
0.186	0.233
0.186	0.263
0.186	0.245
0.186	0.220
0.791	0.702
0.791	0.668
0.791	0.661
0.791	0.721
0.791	0.681

Table 2. Point Estimates of r_1 and r_2 for STY−MMA

temp (°C)	r_1	r_2	data source
20	0.3908	0.5057	this work
40	0.5384	0.4797	Fukuda et al.[4]
40	0.4795	0.4198	Maxwell et al.[18] (composition)
40	0.5212	0.4648	Maxwell et al.[18] (sequence distribution)
60	0.4706	0.5338	Burke et al.[20]
60	0.4719	0.4535	O'Driscoll et al.[21] (kinetic NMR)
overall	0.4890	0.4929	this work (combined data)

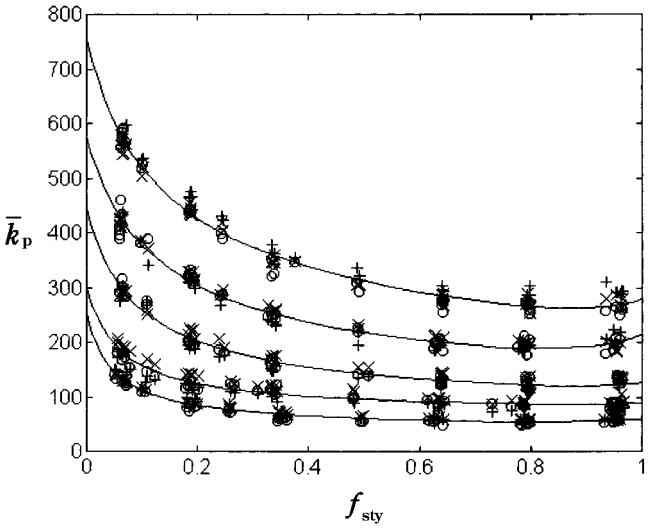

Figure 2. $\bar{k}_p$ data for all temperatures (17.9, 27.7, 37.6, 47.4, and 57.2 °C). The data from the LALLS (+), DV (○), and DRI (×) are shown separately. The curves are for the implicit penultimate model, as fitted to the combined data at each temperature.

Table 3. Homopropagation Rate Coefficients for STY and MMA

temp (°C)	$\bar{k}_p$ of STY [(L/mol)/s]	$\bar{k}_p$ of MMA [(L/mol)/s]
17.9	59.8	250.9
27.7	89.2	299.8
37.6	127.0	446.0
47.4	215.0	576.0
57.2	279.1	756.3

Table 4. Point Estimates of the Radical Reactivity Ratios of STY−MMA

temp (°C)	DRI	LALLS	DV	combined
17.9	$s_1 = 0.4785$	$s_1 = 0.3666$	$s_1 = 0.3406$	$s_1 = 0.3951$
	$s_2 = 0.1643$	$s_2 = 0.2264$	$s_2 = 0.1791$	$s_2 = 0.1827$
27.7	$s_1 = 0.5116$	$s_1 = 0.4110$	$s_1 = 0.5850$	$s_1 = 0.4964$
	$s_2 = 0.2391$	$s_2 = 0.1975$	$s_2 = 0.1537$	$s_2 = 0.1912$
37.6	$s_1 = 0.4606$	$s_1 = 0.3033$	$s_1 = 0.3669$	$s_1 = 0.3708$
	$s_2 = 0.2971$	$s_2 = 0.6973$	$s_2 = 0.4246$	$s_2 = 0.4072$
47.4	$s_2 = 0.3310$	$s_1 = 0.3022$	$s_1 = 0.2968$	$s_1 = 0.3094$
	$s_2 = 0.5902$	$s_2 = 0.5775$	$s_2 = 0.8934$	$s_2 = 0.6611$
57.2	$s_1 = 0.3637$	$s_1 = 0.4218$	$s_1 = 0.3081$	$s_1 = 0.3615$
	$s_2 = 0.5348$	$s_2 = 0.4720$	$s_2 = 1.1183$	$s_2 = 0.6014$

MMA. It was thought that an upper bound to the temperature effect on the monomer reactivity ratios (in the range 20−60 °C) could then be estimated from the uncertainty in these overall reactivity ratios, as measured by the 95% JCI. The additional uncertainty in the radical reactivity ratios, caused by using the same monomer reactivity ratios at all temperatures, could then be estimated using sensitivity analysis. The monomer reactivity ratios obtained from the overall analysis were $r_1 = 0.4890$ and $r_2 = 0.4929$, and a 95% JCI for these values is included (in bold) in Figure 1. It should be noted that the data of O'Driscoll et al.[19] were not included in the analysis as the assumption of negligible error in the independent variable was not valid for this conversion dependent data, and hence it could not be analyzed using the same statistical procedure as the other data sets. However, it may be noted that the 95% JCI for the kinetic NMR reactivity ratios from these data is wholly contained within the JCI for the overall analysis of this work.

Implicit Penultimate Model. In this section we fit the implicit penultimate model to our previously published k_p data, in order to estimate the radical reactivity ratios for STY−MMA and examine their temperature dependence. The $\bar{k}_p$ data used may be found in our original paper[1] and will not be reproduced here; however, a plot of these data is provided in Figure 2. Unless otherwise stated, the monomer reactivity ratios used are the values measured in the overall analysis above ($r_1 = 0.4890$ and $r_2 = 0.4929$) and the homopropagation rate coefficients used are those listed in Table 3. These homopropagation rate coefficients are the averages of the values measured in our previous paper, except for the homopropagation rate coefficient of MMA at 47.6 °C—which is the average of the $\bar{k}_p$ values for MMA at this temperature published by Zammit et al.[23]

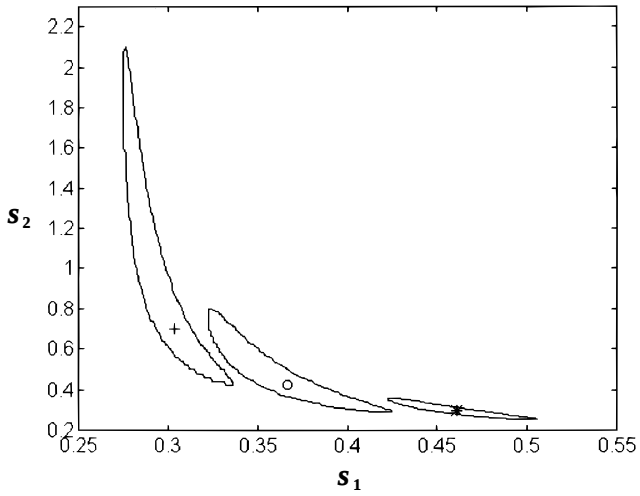

Figure 3. 95% JCIs for the radical reactivity ratios of STY−MMA at 37.6 °C, as fitted separately to the DRI (*), LALLS (+), and DV (○) data.

The analysis is in three parts: (1) a comparison of the radical reactivity ratios obtained from sets of $\bar{k}_p$ data measured at the same temperature but using different molecular weight analysis methods; (2) a comparison of the radical reactivity ratios measured from the combined $\bar{k}_p$ data sets at each temperature; (3) an examination of the temperature effect on the "average" radical reactivity ratio ($s = s_1 = s_2$) obtained from a one-parameter analysis of the combined $\bar{k}_p$ data sets at each temperature, as recommended by Fukuda et al.[3]

Comparison of the Data from the Different Molecular Weight Analysis Methods. As noted above, for each PLP sample there are three estimates of $\bar{k}_p$ (corresponding to the three different methods for measuring molecular weight: LALLS, DV, and DRI). Initially, the data from these three different techniques were analyzed separately, in order to examine the differences between them. The point estimates for the radical reactivity ratios obtained are listed in Table 4, and, as an example, the 95% JCIs for the radical reactivity ratios estimated from the 37.6 °C data sets are given in Figure 3. (The JCIs for the other radical reactivity ratios are provided in the Supporting Information). Examining the JCIs in Figure 3, it is evident that the different data sets give different estimates of the radical reactivity ratios. This suggests that there are systematic errors in the different molecular weight analysis methods. However, as seen in Figure 2, these systematic differences between the data sets are not noticeable in the $\bar{k}_p$ data itself; nor, as shown previously,[1] are they noticeable in the raw molecular weight data from which the $\bar{k}_p$ values were calculated. Furthermore, the relative differences between the radical reactivity ratios obtained from the LALLS, DV, and DRI

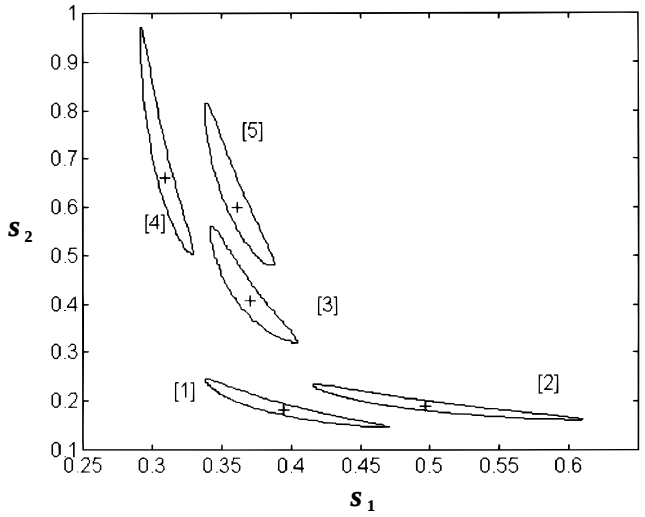

Figure 4. 95% JCIs for the radical reactivity ratios of STY−MMA at 17.9°C [1], 27.7 °C [2], 37.6 °C [3], 47.4 °C [4], and 57.2 °C [5], as fitted to the combined data.

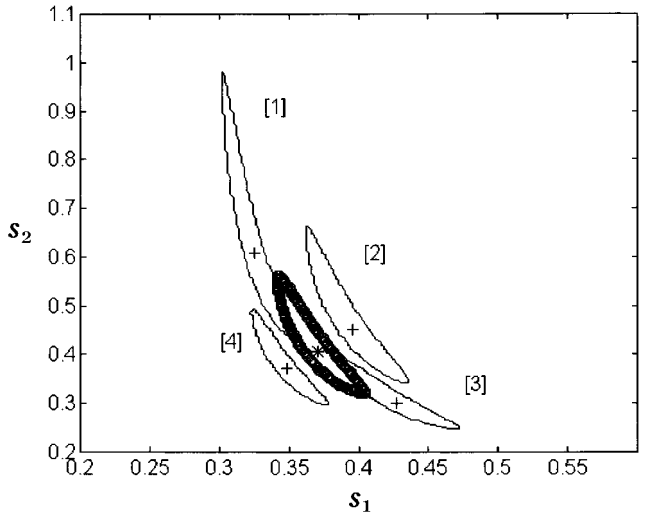

Figure 5. Effect of the homopropagation rate coefficient on the 95% JCIs for the radical reactivity ratios of STY−MMA at 47.4 °C, as fitted separately to the combined data.

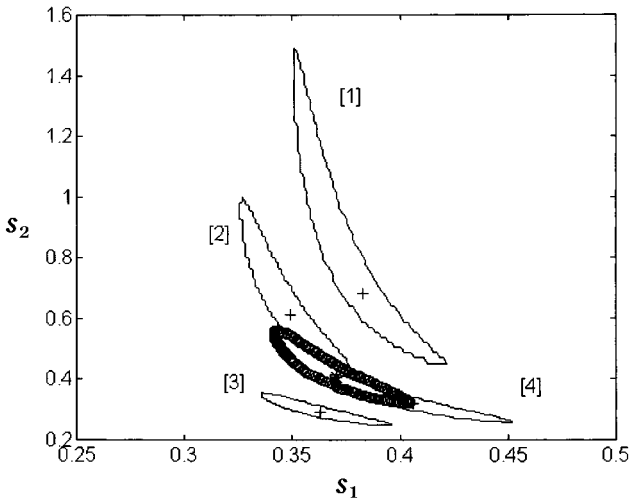

Figure 6. Effect of the monomer reactivity ratios on the 95% JCIs for the radical reactivity ratios of STY−MMA at 47.4 °C, as fitted separately to the combined data.

data sets are not constant with temperature. Hence, it seems that the differences between the radical reactivity ratios that are estimated from the different data sets are not caused by some calibration error in the molecular weight analysis but merely by the amplification of small statistical differences between the three data sets. This highlights a central difficulty in obtaining accurate and precise values of the radical reactivity ratios: the fact that these parameters are extremely sensitive to small variations in the data.

Temperature Effects on Radical Reactivity Ratios. Since it was not possible to establish which of the individual data sets produced the most accurate radical reactivity ratios, the data sets were combined and the radical reactivity ratios were estimated from the combined data at each temperature. The point estimates for the radical reactivity ratios obtained from this analysis are included in Table 4, and their 95% JCIs are plotted in Figure 4. Examining these data, we found no temperature trend in the s_1 values but it appears that the s_2 values approach unity as the temperature increases.

However, this apparent trend in the s_2 values disappears when the sensitivity analysis is performed. Taking the data at the central temperature (37.6 °C), the 95% JCIs for s_1 and s_2 were recalculated for four different combinations of homopropagation rate coefficients, and then for four different combinations of reactivity ratios. The homopropagation rate coefficients (in (L/mol)/s) selected for the sensitivity analysis were [1] $k_{111} = 133.4$ and $k_{222} = 423.7$, [2] $k_{111} = 120.7$ and $k_{222} = 423.7$, [3] $k_{111} = 120.7$ and $k_{222} = 468.3$, and [4] $k_{111} = 133.4$ and $k_{222} = 468.3$. These values correspond to all combinations of the values that are ±5% of the original values. The 95% JCIs obtained for the different combinations of homopropagation rate coefficients, together with the original 95% JCI, are plotted in Figure 5. Examining this figure it is seen that the JCIs span most of the region covered by the original JCIs for the radical reactivity ratios at the different temperatures. Hence, if the uncertainty in the homopropagation rate coefficients is taken into account, the true uncertainty in the radical reactivity ratios renders the apparent temperature trends statistically insignificant.

A similar result is obtained when sensitivity analysis on the monomer reactivity ratios is performed. The monomer reactivity ratios, selected from within the 95% JCI for the overall analysis of the composition and sequence distribution data, were [1] $r_1 = 0.60$ and $r_2 = 0.50$, [2] $r_1 = 0.50$ and $r_2 = 0.43$, [3] $r_1 = 0.40$ and $r_2 = 0.50$, and [4] $r_1 = 0.50$ and $r_2 = 0.56$. The 95% JCIs obtained for the different pairs of monomer reactivity ratios, together with the original 95% JCI, are plotted in Figure 6. Examining this figure, one sees that the JCIs span most of the region covered by the original JCIs for the radical reactivity ratios at the different temperatures. Hence, if the uncertainty in the monomer reactivity ratios is taken into account, the true uncertainty in the radical reactivity ratios renders the apparent temperature trends statistically insignificant.

Although there are no statistically significant temperature trends in the radical reactivity ratios, it does not necessarily follow that there are no temperature effects at all. Within these 95% JCIs physically significant temperature trends are possible. For instance, based on these results, the values of the s_1 parameter in the temperature range 17.9−57.2 °C lie between 0.3 and 0.5. Now, if we suppose that the true value of s_1 was 0.5 at 17.9 °C and 0.3 at 57.2 °C, this would correspond to an activation energy difference (between the homopropagation step of STY, and the same reaction

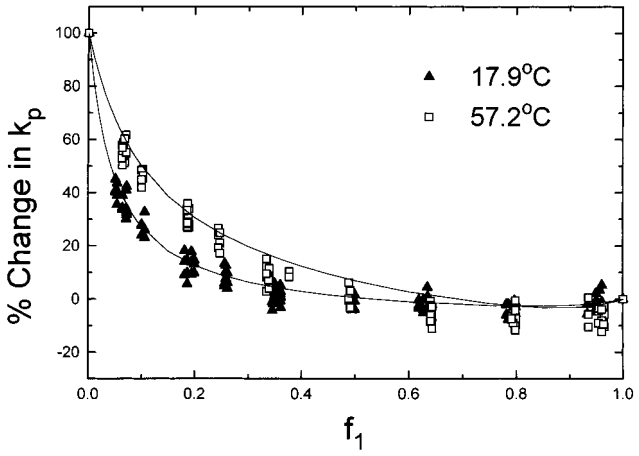

Figure 7. Scaled $\bar{k}_p$ data for STY−MMA at 17.9 and 57.2 °C. The curves are the scaled implicit penultimate model fits.

but with an MMA penultimate unit) of around 10 kJ/mol—which is as big as the activation energy difference between a STY and an MMA homopropagation step and therefore physically unrealistic. For the s_2 value, even larger effects are possible. Hence, at a 95% level of confidence, it is impossible to discriminate between the following types of temperature dependence for the radical reactivity ratios of STY−MMA: no temperature effect (consistent with the entropic model); a small temperature effect (consistent with the enthalpic model); or an unrealistically large temperature effect (inconsistent with both the enthalpic and entropic models). Given this problem, it can be concluded that the uncertainty in the radical reactivity ratios precludes the attachment of any physical significance to their point estimates. Furthermore, this uncertainty in the radical reactivity ratios seems to be unavoidable, given their extreme sensitivity to small changes in the $\bar{k}_p$ data, and to the values of the homopropagation rate coefficients and monomer reactivity ratios that are used in the analysis. It thus appears that *physically meaningful radical reactivity ratios cannot be measured from* $\bar{k}_p$ *data.*

Temperature Effects on the "Average" Radical Reactivity Ratios. Given the problem with measuring physically meaningful radical reactivity ratios, we examined the $\bar{k}_p$ data directly for any qualitative change in the shape of the $\bar{k}_p$ curves with temperature. It was thought that, since the presence of a penultimate unit effect tends to decrease the $\bar{k}_p$ of a copolymerization below its terminal model prediction, any change in the depth of the $\bar{k}_p$ curves with temperature might indicate a change in the magnitude of the penultimate unit effects. In order to compare the shape of the curves at the different temperatures, all of the $\bar{k}_p$ data were rescaled so that it was represented as a percentage of the total change in the homopolymerization rate coefficients at their respective temperatures. When this was done, it was found that the $\bar{k}_p$ curves did become progressively shallower as the temperature increased, as seen in the plot of the scaled data that is given in Figure 7. For the sake of clarity, only the data at the highest and lowest temperatures have been plotted; however, the data at the intermediate temperatures do vary regularly between these two extremes. On the basis of this result, it appears that there may be a small temperature effect on the copolymerization behavior of STY−MMA.

In order to quantify this qualitative trend in the $\bar{k}_p$ data, the combined data at each temperature were fitted for values of the "average" radical reactivity ratio ($s = s_1 = s_2$) using the one parameter analysis method suggested by Fukuda et al.[3] Although the average s values obtained from this analysis are not physically meaningful, they nevertheless provide a measure of the deviation of the $\bar{k}_p$ data from the predictions of the terminal model. The average s values obtained by fitting this one-parameter equation to the combined $\bar{k}_p$ data at each temperature are given in Table 5. The point estimates and their 95% confidence interval were obtained using the homopropagation rate coefficients from Table 3 and the overall monomer reactivity ratios ($r_1 = 0.4890$ and $r_2 = 0.4929$). Sensitivity analysis was performed on the data at each temperature using all possible combinations of ±5% of their respective homopropagation rate coefficients and the same four additional monomer reactivity ratio pairs that were used in the sensitivity analysis of the s_1 and s_2 values, as detailed above. The resulting overall 95% confidence intervals for the s values at these three temperatures are also included in Table 5. Examining the data in Table 5, it is evident that there is a small temperature effect on the average s values and, at a 95% level of confidence, this temperature effect is *statistically significant,* even after the uncertainties in the monomer reactivity ratios and homopropagation rate coefficients are taken into account. Hence it appears that the implicit penultimate unit effect—at least in the system STY−MMA—does contain an enthalpic component.

Table 5. Average Radical Reactivity Ratios of STY−MMA

temp (°C)	s value (point estimate)	95% CI (optimum parameters)	95% CI (sensitivity analysis)
17.9	0.311	0.304−0.318	0.269−0.359
27.7	0.340	0.331−0.350	0.295−0.393
37.6	0.379	0.372−0.386	0.334−0.433
47.4	0.365	0.359−0.371	0.328−0.412
57.2	0.410	0.403−0.417	0.366−0.467

Terminal Bootstrap Model. As we noted in the Introduction to this paper, previous attempts at discrimination between the implicit penultimate model and the terminal bootstrap model have not been successful because these models have several adjustable parameters and, by selection of appropriate values of these parameters, both models can be made to fit existing copolymerization data. It is for this reason that, in this work, we have been evaluating the alternative copolymerization models by examining the physical significance of the model parameters rather than merely the ability of the model to fit the data. Now, in the bootstrap model there are three adjustable parameters in the composition and triad fraction equations (the two reactivity ratios, r_1 and r_2, and the equilibrium constant, K) and the same three adjustable parameters appear in the $\bar{k}_p$ equation. The $\bar{k}_p$ equation also contains the homopropagation rate coefficients (k_{111} and k_{222}) but these can be measured independently of copolymerization data and thus are not really "adjustable" parameters (although their uncertainty must still be considered in the overall uncertainty of the fitted model parameters). So, unlike the implicit penultimate model, in the bootstrap model the same set of adjustable parameters appear in both the composition and $\bar{k}_p$ equations. Hence, although we cannot critically test the model by merely examining its fit to either set of data, it may be possible to critically test the model by fitting it to one data set (composition or $\bar{k}_p$) and using the

Table 6. Bootstrap Model Parameters from $\bar{k}_p$ Data

temp (°C)	r_1	r_2	K	SS
17.9	0.026	9.86	19.1	3360
	2.35	0.11	0.21	
27.7	−0.024	7.13	18.8	2563
	2.12	−0.081	−0.214	
37.6	−0.021	7.75	12.1	2485
	2.21	−0.074	−0.12	
47.4	0.019	6.56	8.44	3916
	2.45	0.050	0.064	
57.2	0.048	5.96	7.26	1896
	2.20	0.13	0.16	

parameters obtained to predict the behavior of the other data set, which can then be compared with measured values. Therefore, in this section we first fit the terminal bootstrap model to the $\bar{k}_p$ data and, using the parameters obtained, test the bootstrap model predictions against available composition data. Following this, we further test the bootstrap model by examining the physical significance of the parameters obtained. Finally, we examine the literature for evidence for and against the physical basis of a bootstrap effect in STY−MMA.

Model Fitting Results. The terminal bootstrap model was fitted to the combined $\bar{k}_p$ data at each temperature. The homopropagation rate coefficients were fixed at the values listed in Table 3, and only the parameters r_1, r_2, and K were varied in minimizing the weighted sum of squares. In performing the analysis we found that not only were there many local minima in the SS surface but also there were multiple global minima. To ensure that all of these global minima (within a specified range) were detected, the regression analysis of each data set was performed for 15 625 different sets of initial parameter estimates. These sets were formed from all possible combinations of values of each parameter in the range 0.1−5.1 with a step size of 0.2. At each temperature, two parameter sets produced the overall minimum SS (within a tolerance of 1 unit) and these are listed in Table 6.

Using the parameters measured from the $\bar{k}_p$ data, the bootstrap model prediction of the composition curve for STY−MMA was obtained. These predicted values were then compared with the predictions of the terminal model (using the overall reactivity ratios, $r_1 = 0.4890$ and $r_2 = 0.4929$) and the available composition data (the 20 °C data measured in this work, together with the 40 °C data of Fukuda et al.[4] and Maxwell et al.[18]). It was found that the parameters measured from the 20 °C $\bar{k}_p$ data adequately described all of the composition data and, for these parameters, there was no discernible difference between the predictions of the bootstrap model and the terminal model. However, the parameters measured at the higher temperatures failed to describe the composition of STY−MMA and, based on this result, it would appear that the bootstrap model cannot simultaneously describe the composition and $\bar{k}_p$ of STY−MMA at these higher temperatures. However, this is not necessarily the case—since there may exist parameters that, while not providing the "best fit" to either individual data set, nevertheless adequately describe both the composition and $\bar{k}_p$ data. For instance, the parameters obtained by Maxwell et al.[18] by simultaneously fitting the bootstrap model to the 40 °C composition and $\bar{k}_p$ data of Fukuda et al.[4] predict (using the homopropagation rate coefficients of Table 3) $\bar{k}_p$ values that are reasonably close to those measured in this work (the deviation only just exceeding the scatter in the data). Hence, it is likely that parameters could be found so that the composition and $\bar{k}_p$ data of STY−MMA is simultaneously described by the bootstrap model, and the model should be simultaneously fitted to both data sets before any firm conclusions are drawn.

Physical Significance of the Parameters. It therefore appears that it is necessary to simultaneously fit the composition and $\bar{k}_p$ data in order to obtain the correct estimates of the bootstrap model parameters. However, for this work, simultaneous fitting was not possible because composition data for STY−MMA were not available at each temperature. If a single set of composition data was used at each temperature, and the temperature dependence of the composition data was thereby ignored, this temperature dependence would appear as a systematic error in the bootstrap model parameters, and might be mistaken for a temperature effect. This problem is analogous to that of correcting for the temperature dependence of the monomer reactivity ratios when measuring the temperature dependence of the radical reactivity ratios in the implicit penultimate model. While, for the implicit penultimate model, qualitative results could be obtained by correcting for the temperature dependence of the monomer reactivity ratios through sensitivity analysis, such an approach is not possible for the bootstrap model, as the sensitivity analysis would need to involve a data set rather than merely a parameter set. For these reasons, the model was not fitted simultaneously to the composition and $\bar{k}_p$ data and thus the temperature dependence of the fitted model parameters could not be examined.

However, the parameters measured from the 20 °C data do simultaneously fit the composition and $\bar{k}_p$ data of STY−MMA. Hence these parameters could be treated as good estimates of the bootstrap model parameters at 20 °C. Examining the point estimates at this temperature, it is seen that the monomer reactivity ratio pairs obtained consist of one parameter that is very close to zero (and possibly negative) and the other much greater than one. In contrast, the monomer reactivity ratios of STY−MMA that are (directly) measured using end-group studies are around 0.5 for each monomer[24]—similar to those measured by fitting the terminal model to composition data. Hence, it would appear that the fitted model parameters of the bootstrap model are not physically realistic. The validity of this conclusion was checked by calculating the 95% JCI for the parameters and correcting this JCI for the uncertainty in the homopropagation rate coefficients (within ±5%) through sensitivity analysis. Owing to the difficulty in representing a three-dimensional figure in two dimensions clearly, the resulting JCI has not been reproduced here. However, it was found that, even when the uncertainty in the fitted model parameters was taken into account, values of r_1 and r_2 still fell into the range $r_1 \approx 0$ and $r_2 \gg 1$ or vice versa. Furthermore, the JCI obtained could be considered to be an overestimate rather than underestimate of the true uncertainty in the parameters, since it failed to take into account the fit of the model to the composition data. Hence we can conclude with a reasonable degree of certainty that, according to the bootstrap model, the true monomer reactivity ratios of STY−MMA are either $r_1 \approx 0$ and $r_2 \gg 1$ or vice versa—values that appear to be physically unrealistic.

Evidence against a Bootstrap Effect in STY−MMA. Given this apparent failure of the bootstrap

Table 7. Average Activation Energy and Frequency Factors for STY−MMA

f_1 (STY)	E_{act} (kJ/mol)	log(*A*)
0	22.33	6.425
0.064	30.9	7.645
0.11	32.9	7.928
0.19	34.1	8.053
0.25	33.8	7.953
0.34	34.3	7.975
0.49	33.4	7.782
0.64	32.1	7.530
0.79	33.5	7.739
0.95	31.6	7.442
1	32.51	7.630

model, we examined the literature for studies that directly tested its physical grounds. The possible causes of a bootstrap effect in a bulk copolymerization such as STY−MMA include nonideal mixing of the comonomers, complex formation between the monomers and chain end, or preferential solvation of the growing polymer chains by one of the monomers. In examining the literature we found experimental evidence against each of these possible causes in the system STY−MMA. Nonideal mixing in this system was discounted by Semchikov et al.,[25] who calculated the total and excess thermodynamic functions of mixing for the comonomers STY−MMA from measurements of their solution thermodynamics. They found that this system had very small negative ΔG^E values over the temperature range tested (298−343 K) and hence could be considered to form comonomer solutions that were close to ideality. Complex formation between the monomer and growing polymer radicals for STY−MMA was discounted by Fukuda et al.[26] They measured the k_p of the system STY−MMA in a solution of 50% toluene (TOL) and found that the kinetic behavior was similar to that of bulk STY−MMA. They argued that, since the presence of a third solvent would proportionally decrease the concentration of the complex to that of the free monomer, had complexation been important in determining the copolymerization kinetics of STY−MMA, the kinetics of STY−MMA-TOL should have been different. Finally, studies of polymer−solvent interaction parameters by Kamachi[27] and Kratochvil et al.[28] indicate that preferential solvation of the polymer chains by one of the monomers is unlikely to be significant for bulk STY−MMA. On the basis of this survey of the literature, it can be concluded that there is strong evidence against the obvious sources of a bootstrap effect in the copolymerization kinetics of bulk STY−MMA. Therefore, it is unlikely that this model is a genuine alternative to the implicit penultimate model for describing the kinetics of ordinary copolymerizations such as STY−MMA.

Activation Energies and Frequency Factors. As the $\bar{k}_p$ of STY−MMA was measured as a function of both monomer feed ratio and temperature, it was possible to estimate the Arrhenius parameters for STY−MMA copolymerizations at the different temperatures. The Arrhenius relationship was fitted to the combined $\bar{k}_p$ data, and estimates for the average activation energy and frequency factors at each monomer feed ratio were obtained. The point estimates of these Arrhenius parameters are given in Table 7, together with the IUPAC benchmark values for the homopolymerization of MMA[29] and STY.[30] The 95% joint confidence intervals for each set of Arrhenius parameters were calculated, but owing to lack of space, they have not been reproduced here. However, the uncertainty in the sets

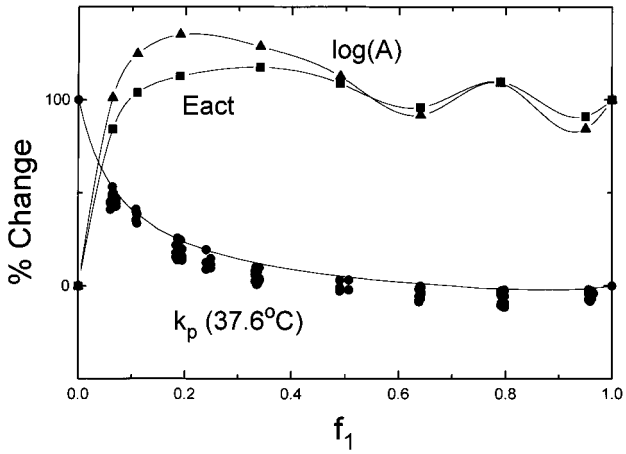

Figure 8. Scaled activation energies and frequency factors, together with the scaled 37.6 °C k_p values. The curve fitted to the $\bar{k}_p$ data is the scaled implicit penultimate model fit. The curves through the activation energy and frequency factors are not from any model; the points are joined merely for clarity.

of Arrhenius parameters may be summarized as follows. The uncertainty in the activation energies was no more than ±2 kJ/mol, the uncertainty in the frequency factors was no more than $\pm 10^7$ (L/mol)/s, and the uncertainty in both parameters was highly correlated.

Two observations may be made concerning this data. Firstly, the Arrhenius relationship provided a good description of the data. This fit could not be quantified using a "goodness-of-fit" test, as it was difficult to estimate the experimental error in the data for such small numbers of replicates. However, when the model predictions and measured data were compared, it was seen that the model closely described the data. Given this ability of the Arrhenius model to describe the $\bar{k}_p$ of different STY−MMA copolymerizations, it is not likely that the behavior is being complicated by a solvent effect (such as partitioning or complex formation), although, given the relatively narrow temperature range under study and the complex nature of the kinetic models, model discrimination upon this basis is perhaps unwise. Hence it appears (by default) that the kinetic behavior of STY−MMA is likely to be caused by a penultimate unit effect.

Secondly, when the Arrhenius parameters are plotted as a percentage of the difference between their homopolymerization values, both the activation energy and frequency factor vary in a similar manner, and this behavior mirrors the behavior of $\bar{k}_p$ (though in an inverse manner). To illustrate this, a plot of these scaled activation energies and frequency factors is given in Figure 8. For comparison, the scaled $\bar{k}_p$ data at 37.6 °C are also plotted. Examining the plot, we see that the activation energies and frequency factors jump to more than 80% of the STY homopropagation values after the addition of only 6.4 mol % of STY. At the same time, the $\bar{k}_p$ values drop to 50% of their MMA homopropagation values. Hence, as in the case of $\bar{k}_p$, a small addition of STY causes a proportionally large change in both the frequency factor and activation energy. Given this behavior, it would qualitatively appear that there is a penultimate unit effect in both activation energy and frequency factor. It should be noted that this result is statistically significant, since the change in activation energy and frequency factor between $f_1 = 0$ and $f_1 = 0.064$ greatly exceeds the maximum uncertainty in the parameters; however, the

smaller variation of these Arrhenius parameters at higher concentrations of STY lies within the limits of experimental error.

These results thus indicate (by default) the presence of a penultimate unit effect in STY−MMA copolymerizations and appear to suggest that this penultimate unit effect contains both an entropic and an enthalpic component. However, when expressions for the average activation energy and frequency are derived, it can be seen that the behavior observed above is in fact consistent with (1) a penultimate unit effect in both activation energy and frequency factor (general case), (2) a penultimate unit effect only in activation energy (enthalpic model), and (3) a penultimate unit effect only in frequency factor (entropic model). In what follows, we derive expressions for the average activation energy and frequency factor for these different cases and show how these different cases could give rise to the behavior seen above.

(1) General Case. The Arrhenius parameters for the propagation step of a free-radical copolymerization may be expressed as the weighted sum of the individual Arrhenius parameters. Each term is weighted according to the probability of that step occurring, that is, by the ratio of the reaction rate for that step to the overall propagation rate. For a system in which penultimate unit effects are important, the average activation energy and frequency factor may be defined as follows.

$$\bar{E} = \sum_{i=1}^{2}\sum_{j=1}^{2}\sum_{k=1}^{2}\left(\frac{r_{pijk}}{r_p}\right)E_{ijk} = \sum_{i=1}^{2}\sum_{j=1}^{2}\sum_{k=1}^{2}\left(\frac{k_{pijk}}{k_p}f_k\frac{[M_iM_j^\bullet]}{[R^\bullet]}\right)E_{ijk} \tag{17}$$

$$\bar{A} = \sum_{i=1}^{2}\sum_{j=1}^{2}\sum_{k=1}^{2}\left(\frac{r_{pijk}}{r_p}\right)A_{ijk} = \sum_{i=1}^{2}\sum_{j=1}^{2}\sum_{k=1}^{2}\left(\frac{k_{pijk}}{k_p}f_k\frac{[M_iM_j^\bullet]}{[R^\bullet]}\right)A_{ijk} \tag{18}$$

where r_{pijk} is the propagation rate for the reaction of $M_iM_j^\bullet$ with M_k, r_p is the overall propagation rate, k_{pijk} is the propagation rate coefficient for the reaction of $M_iM_j^\bullet$ with M_k, k_p is the overall propagation rate coefficient, f_k is the molar fraction of M_k in the feed, $[R^\bullet] = [M_1M_1^\bullet] + [M_2M_1^\bullet] + [M_1M_2^\bullet] + [M_2M_2^\bullet]$, E_{ijk} is the activation energy for the reaction of $M_iM_j^\bullet$ with M_k and A_{ijk} is the frequency factor for the reaction of $M_iM_j^\bullet$ with M_k.

Assuming an implicit penultimate unit effect, but making no assumptions as to its origin, expressions for the relative radical concentrations were derived. These expressions are as follows:

$$\frac{[M_1M_1^\bullet]}{[R^\bullet]} = \frac{1}{1 + \frac{[M_2M_1^\bullet]}{[M_1M_1^\bullet]} + \frac{[M_1M_2^\bullet]}{[M_1M_1^\bullet]} + \frac{[M_2M_2^\bullet]}{[M_1M_1^\bullet]}} \tag{19}$$

$$\frac{[M_1M_2^\bullet]}{[R^\bullet]} = \frac{\frac{[M_1M_2^\bullet]}{[M_1M_1^\bullet]}}{1 + \frac{[M_2M_1^\bullet]}{[M_1M_1^\bullet]} + \frac{[M_1M_2^\bullet]}{[M_1M_1^\bullet]} + \frac{[M_2M_2^\bullet]}{[M_1M_1^\bullet]}} \tag{20}$$

$$\frac{[M_2M_1^\bullet]}{[R^\bullet]} = \frac{\frac{[M_2M_1^\bullet]}{[M_1M_1^\bullet]}}{1 + \frac{[M_2M_1^\bullet]}{[M_1M_1^\bullet]} + \frac{[M_1M_2^\bullet]}{[M_1M_1^\bullet]} + \frac{[M_2M_2^\bullet]}{[M_1M_1^\bullet]}} \tag{21}$$

$$\frac{[M_2M_2^\bullet]}{[R^\bullet]} = \frac{\frac{[M_2M_2^\bullet]}{[M_1M_1^\bullet]}}{1 + \frac{[M_2M_1^\bullet]}{[M_1M_1^\bullet]} + \frac{[M_1M_2^\bullet]}{[M_1M_1^\bullet]} + \frac{[M_2M_2^\bullet]}{[M_1M_1^\bullet]}} \tag{22}$$

where

$$\frac{[M_2M_1^\bullet]}{[M_1M_1^\bullet]} = \frac{f_2}{f_1r_1s_1}$$

$$\frac{[M_1M_2^\bullet]}{[M_1M_1^\bullet]} = \frac{f_2r_2k_{111}(f_1r_1 + f_2)}{f_1r_1^2s_2k_{222}(f_1 + f_2r_2)}$$

$$\frac{[M_2M_2^\bullet]}{[M_1M_1^\bullet]} = \frac{(r_2f_2)^2k_{111}(f_1r_1 + f_2)}{(f_1r_1)^2k_{222}(f_1 + f_2r_2)}$$

It should be noted that although the individual activation energies and frequency factors are not temperature dependent, the average quantities are temperature dependent through the radical concentrations and propagation rate constants that weight the contributions of the individual quantities. This temperature dependence invalidates the Arrhenius expression since this expression assumes that the activation energy and frequency factor are constant with temperature. However, given the fact that the Arrhenius model was successfully fitted to the data, it appears that this temperature dependence was not significant for STY−MMA over the temperature range studied. This observation is in keeping with our earlier observation concerning the apparent insensitivity to temperature of the monomer reactivity ratios.

(2) Enthalpic Model. If we assume that the penultimate unit effect is entirely enthalpic, the original equation for the average activation energy stands. However, the equation for the average frequency factor may be simplified, as follows. Since there is no penultimate unit effect in frequency factor, the following equalities hold:

$$A_{211} = A_{111} = A_{11};\ A_{212} = A_{112} = A_{12};\ A_{122} = A_{222} = A_{22};\ A_{121} = A_{221} = A_{21}$$

With this simplification, the equation for the average frequency factor becomes

$$\bar{A} = \sum_{j=1}^{2}\sum_{k=1}^{2}\left(\frac{r_{p1jk} + r_{p2jk}}{r_p}\right)A_{jk} = \sum_{j=1}^{2}\sum_{k=1}^{2}\left(\frac{k_{p1jk} + k_{p2jk}}{k_p}\right)f_k\left(\frac{[M_1M_j^\bullet] + [M_2M_j^\bullet]}{[R^\bullet]}\right)A_{jk} \tag{23}$$

(3) Entropic Model. If we assume that the penultimate unit effect is entirely enthalpic, the original equation for the average frequency factor stands. How-

ever, the equation for the average activation energy may be simplified, as follows. Since there is no penultimate unit effect in activation energy, the following equalities hold:

$$E_{211} = E_{111} = E_{11} \qquad E_{212} = E_{112} = E_{12}$$
$$E_{122} = E_{222} = E_{22} \qquad E_{121} = E_{221} = E_{21}$$

With this simplification, the equation for the average activation energy becomes

$$\bar{E} = \sum_{j=1}^{2}\sum_{k=1}^{2}\left(\frac{r_{p1jk} + r_{p2jk}}{r_p}\right)E_{jk} = \sum_{j=1}^{2}\sum_{k=1}^{2}\left(\frac{k_{p1jk} + k_{p2jk}}{k_p}\right)f_k\left(\frac{[M_1M_j^\bullet] + [M_2M_j^\bullet]}{[R^\bullet]}\right)E_{jk} \quad (24)$$

Model Discrimination. Examining the simplified average activation energy expression for the entropic model, and the simplified average frequency factor for the enthalpic model, it can be seen that although there is no penultimate unit effect in the individual Arrhenius parameters, there is a penultimate unit effect in the radical concentrations and propagation rate coefficients that weight these quantities. Hence it is possible that in both of these cases, the average Arrhenius parameters might still be expected to vary in an inverse manner with $\bar{k}_p$, and thus qualitative model discrimination is not possible. Quantitative model discrimination would be possible if the temperature dependence of the monomer reactivity ratios and point estimates of the radical reactivity ratios were accurately known, since these quantities could then be used to predict the exact behavior expected under the two simplified cases. However, as seen in this work, the accurate and precise estimation of these quantities (at least for a system such as STY−MMA) is difficult and thus unlikely to be achieved in the near future. Furthermore, even if this were possible, the temperature dependence of these average Arrhenius parameters would complicate the model discrimination.

Conclusions

In this work, both the implicit penultimate model and a version of the terminal bootstrap model were fitted to extensive $\bar{k}_p$ data for STY−MMA. The objective of this work was to discriminate between these models by comparing the temperature dependence of their fitted model parameters with that expected given their physical meaning. Unfortunately, this kinetic analysis was inconclusive since accurate composition data (and hence monomer reactivity ratios) at each temperature were not available. This meant that systematic error in the fitted model parameters (from the uncorrected temperature dependence of the composition data or monomer reactivity ratios) could not be ruled out. In the case of the implicit penultimate model, this problem was to some extent addressed through sensitivity analysis; however, the extreme sensitivity of the fitted model parameters to small errors in the data, the monomer reactivity ratios and homopropagation rate coefficients, rendered their accurate and precise estimation impossible. Hence, although no statistically significant trends were observed in the parameters, the uncertainty was too large to rule out physically significant trends.

The average activation energies and frequency factors were also calculated for STY−MMA copolymerizations, and the physical meaning of these parameters was explored. It was found that both the average activation energy and frequency factor varied in a similar manner to $\bar{k}_p$. However, this behavior does not necessarily indicate that the penultimate unit effect has both an enthalpic and entropic component. This is because, even when there is no penultimate unit effect in the individual Arrhenius parameters, a penultimate unit effect appears in the average parameters through the radical concentrations and individual rate coefficients that weight the individual contributions. Hence this data was not useful for discriminating between the enthalpic and entropic models.

Despite these problems, two important observations were made. Firstly, there appears to be a temperature effect on the radical reactivity ratios of STY−MMA. This was based on the qualitative observation that the shape of the $\bar{k}_p$ curves became slightly shallower with temperature, a trend that was confirmed when the $\bar{k}_p$ data were analyzed for a single "average *s* value" and remained even when the uncertainty arising from the possible temperature dependence of the monomer reactivity ratios was taken into account. The presence of a statistically significant temperature effect on this *s* value suggests that there may be an enthalpic component to any penultimate unit effect present. Secondly, it appears that the bootstrap model is not a realistic alternative to the implicit penultimate model for describing the kinetics of ordinary copolymerizations such as STY−MMA. This conclusion was based on a number of observations. Firstly, it was shown that, according to the bootstrap model, the true monomer reactivity ratios of STY−MMA consist of one parameter that is close to zero and the other much greater than one, or vice versa—values that do not appear to be physically realistic. Secondly, the Arrhenius model successfully described the temperature dependence of the $\bar{k}_p$ data—which suggests that the copolymerization behavior is not being complicated by solvent effects such as a bootstrap effect, although this alone is not sufficient for model discrimination. Finally, in a review of the literature we identified experimental evidence against the main sources of a bootstrap effect in the system STY−MMA. Such evidence was based upon more direct examination of the physical grounds of this model, and we recommend this approach for future studies of copolymerization kinetics.

Acknowledgment. We gratefully acknowledge the receipt of a grant from the Australian Research Council, the receipt of an Australian Postgraduate Award to M.L.C., and the staff at the NMR service at the School of Chemistry, at the University of NSW, for performing the NMR analyses.

Supporting Information Available: Plots of 95% JCIs for the radical reactivity ratios of STY−MMA at 17.9, 27.7, 47.4, and 57.2 °C (5 pages). Ordering and access information is given on any current masthead page.

References and Notes

(1) Coote, M. L.; Zammit, M. D.; Davis, T. P.; Willett, G. D. *Macromolecules* ***1997***, *30*, xxxx.
(2) Harwood, H. J. *Makromol. Chem., Macromol. Symp.* **1987**, *10/11*, 331.
(3) Fukuda, T.; Kubo, K.; Ma, Y.-D. *Prog. Polym. Sci.* **1992**, *17*, 875.
(4) Fukuda, T.; Ma, Y.-D.; Inagaki, H. *Macromolecules* **1985**, *18*, 17.

(5) Davis, T. P.; O'Driscoll, K. F.; Piton, M. C.; Winnik, M. A. *J. Polym. Sci., Part C: Polym. Lett.* **1989**, *27*, 181.
(6) Olaj, O. F.; Schnoll-Bitai, I.; Kremminger, P. *Eur. Polym. J.* **1989**, *25*, 535.
(7) Davis, T. P.; O'Driscoll, K. F.; Piton, M. C.; Winnik, M. A. *Macromolecules* **1990**, *23*, 2113.
(8) Davis, T. P.; O'Driscoll, K. F.; Piton, M. C.; Winnik, M. A. *Polym. Int.* **1991**, *24*, 65.
(9) Ma, Y.-D.; Won, Y.-C.; Kubo, K.; Fukuda, T. *Macromolecules* **1993**, *26*, 6766.
(10) Ma, Y.-D.; Kim, D.-S.; Kubo, K.; Fukuda, T. *Polymer* **1994**, *35*, 1375.
(11) Piton, M. C.; Winnik, M. A.; Davis, T. P.; O'Driscoll, K. F. *J. Polym. Sci. Part A, Polym. Chem.* **1990**, *28*, 2097.
(12) Merz, E.; Alfrey, T., Jr.; Goldfinger, G. *J. Polym. Sci.* **1946**, *1*, 75.
(13) Fukuda, T.; Ma, Y.-D.; Kubo, K.; Inagaki, H. *Macromolecules* **1991**, *24*, 370.
(14) Fukuda, T.; Ma, Y.-D.; Inagaki, H. *Makromol. Chem., Rapid Commun.* **1987**, *8*, 495.
(15) Heuts, J. P. A.; Gilbert, R. G.; Maxwell, I. A. *Macromolecules* **1997**, *30*, 726.
(16) Heuts, J. P. A.; Coote, M. L.; Davis, T. P.; Johnston, L. P. M. *ACS Symp. Ser.*, in press.
(17) Moad, G.; Solomon, D. H.; Spurling, T. H.; Stone, R. A. *Macromolecules* **1989**, *22*, 1145.
(18) Maxwell, I. A.; Aerdts, A. M.; German, A. L. *Macromolecules* **1993**, *26*, 1956.
(19) Draper, N. R.; Smith, H. *Applied Regression Analysis*; John Wiley & Sons: New York, 1981.
(20) Burke, A. L.; Duever, T. A.; Penlidis, A. *J. Polym. Sci., Part A: Polym. Chem.* **1996**, *34*, 2665.
(21) O'Driscoll, K. F.; Kale, L. T.; Garcia Rubio, L. H.; Reilly, P. M. *J. Polym. Sci. Polym. Chem. Ed.* **1984**, *22*, 2777.
(22) Tidwell, P. W.; Mortimer, G. A. *J. Polym. Sci.* **1965**, *A3*, 369.
(23) Zammit, M. D.; Coote, M. L.; Davis, T. P.; Willett, G. D. *Macromolecules*, submitted for publication.
(24) Lyons, R. A.; Senogles, E. *Aust. J. Chem.* **1994**, *47*, 2201.
(25) Semchikov, Y. D. *Polym. Sci. USSR* **1990**, *32*, 177.
(26) Fukuda, T.; Kubo, K.; Ma, Y.-D.; Inagaki, H. *Polym. J. (Tokyo)* **1987**, *19*, 523.
(27) Kamachi, M. *Adv. Polym. Sci.* **1981**, *38*, 56.
(28) Kratochvil, P.; Strakova, D.; Stejskal, J.; Tuzar, Z. *Macromolecules* **1983**, *16*, 1136.
(29) Beuermann, S.; Buback, M.; Davis, T. P.; Gilbert, R. G.; Hutchinson, R. A.; Olaj, O. F.; Russell, G. T.; Schweer, J.; van Herk, A. M. *J. Macromol. Chem. Phys.* **1997**, *198*, 1545.
(30) Buback, M.; Gilbert, R. G.; Hutchinson, R. A.; Klumperman, B.; Kuchta, F.-D.; Manders, B. G.; O'Driscoll, K. F.; Russell, G. T.; Schweer, J. *J. Macromol. Chem. Phys.* **1995**, *196*, 3267.

MA971052K